LM-06K104
October 2, 2006

Development of Front Surface, Spectral Control Filters with Greater Temperature Stability for Thermophotovoltaic Energy Conversion

TD Rahmlow, Jr., DM DePoy, PM Fourspring,
H Ehsani, JE Lazo-Wasem and EJ Gratiix

Development of Front Surface, Spectral Control Filters with Greater Temperature Stability for Thermophotovoltaic Energy Conversion

Thomas D. Rahmlow, Jr.[1], David M. DePoy[2], Patrick M. Fourspring[2], Hassan Ehsani[2], Jeanne E. Lazo-Wasem[1] and Edward J. Gratrix[1]

[1] Rugate Technologies, Incorporated, 353 Christian Street, Oxford, CT USA 06478
[2] Lockheed Martin, Corp., PO Box 1072, Schenectady, NY, USA 12301

Corresponding author: Thomas D. Rahmlow Jr., Rugate Technologies, Inc, 353 Christian St, Oxford CT, USA, 06478, tomrahmlow@rugate.com, (203)-267-3154

Abstract

Spectral control is an important consideration in achieving high conversion efficiency with thermophotovoltaic (TPV) energy conversion systems[1]. TPV modules using front surface filters as the primary spectral control device have demonstrated conversion efficiencies in excess of 20%[2] with power densities in excess of 0.4 W/cm^2. The front surface filter we are developing is a short pass, long wavelength reflection filter consisting of an interference filter deposited on a plasma filter. The materials used in the interference filter must exhibit high broad band transmission and good film quality and sufficient temperature stability at the operating temperature of the TPV cells and over any potential temperature excursions that may occur. Three high refractive index materials that offer good potential for use in TPV spectral control filters are antimony selenide (Sb_2Se_3), antimony sulfide (Sb_2S_3), and gallium telluride (GaTe). The highest spectral efficiency has been demonstrated using Sb_2Se_3; however this material develops significant near infrared (NIR, 0.72-2.5μm) absorption at temperatures in excess of 90°C. The other two materials are being developed as high temperature alternatives to Sb_2Se_3. TPV filters using GaTe and Sb_2S_3 have been designed and fabricated, and initial results indicate that GaTe based filters are capable of operation at temperatures of 150°C or greater. Measured performance of TPV filters containing Sb_2Se_3, GaTe and Sb_2S_3 are presented, along with the impact that these have on TPV module performance.

1: Thermophotovoltaics and Spectral Control

Thermophotovoltaic (TPV) cells absorb above band gap photons and release electrons. They operate in the same manner as solar cells, only at infrared wavelengths. Because the photon must have sufficient energy to make the band gap transition, only above band gap photons can be directly converted to electrical energy. For a blackbody radiator, the majority of the radiated energy may be below band gap. Figure 1 plots the black body spectral curve for a radiator at 1100°C. In this example, 76% of the energy is below the band gap for a 0.60eV TPV cell. If below band gap photons are absorbed by the cell, they are converted to heat; and the energy is lost. However, if the below band gap photons are redirected back towards the radiator, they can be recuperated and system efficiency is improved. Figure 2 illustrates the use of a front surface spectral control filter to reflect the below band gap photons and transmit above band gap photons.

Spectral control refers to the means and methods of improving the efficiency of a TPV energy conversion system by emitting only convertible photons and suppressing non-convertible photons from the radiating side and perfectly transmitting convertible photons and reflecting non-convertible photons that reach the TPV cell. There are many different approaches to spectral control. These approaches include spectrally selective emitters that suppress long wavelength photons emitted by the hot radiator[3], back surface reflectors (BSR) comprised of a metal

reflection layer placed behind the cell to reflect all non-absorbed photons back towards the radiator[4], and front surface filters placed between the emitter and cell to reflect long wavelength photons back towards the radiator and pass the short wavelength photons through to the TPV cell[5].

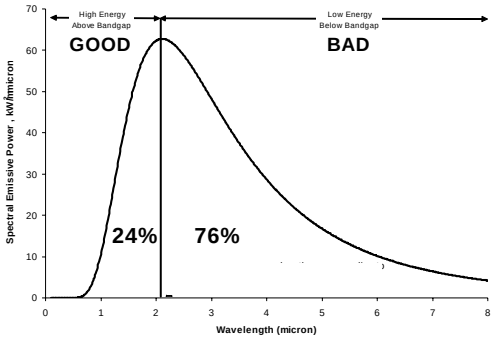

Figure 1: All objects emit light as a function of their temperature and the emissivity of their surface. For a perfect blackbody, the spectral distribution is peaked, but spectrally broad. For a 'perfect' radiator at 1100°C, only 24% of the spectrum is above band gap for a 0.6eV device.

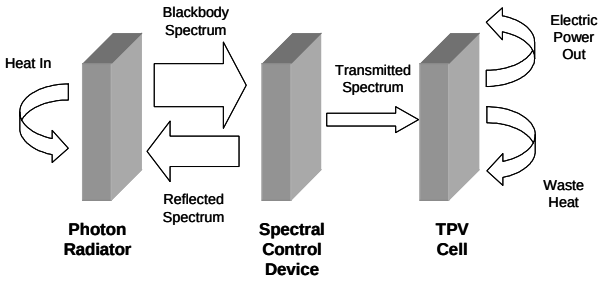

Figure 2: High efficiency in a TPV system requires a spectral control scheme to limit the parasitic loss of below band gap photons. A front surface filter allows above band gap photons to pass through and reflects below band gap photons back towards the radiator.

The specific method of spectral control which we have been developing is a front surface interference filter on a plasma filter. The interference filter is a multilayer film stack of high and low refractive index materials. The interference filter defines the short wavelength transition from high transmission to high reflection at the wavelength of the cell's band gap and provides high reflection in the mid-infrared (MIR, 2-6μm). The plasma filter is a heavily doped semiconductor layer designed to provide long wavelength reflection[6].

Figure 3 illustrates the structure of the front surface filter, plasma filter and index matching layers on the TPV cell or diode. The front surface filter is glued to the cell using an optical adhesive. The physical contact of the filter and diode allows for the cooling of the full assembly from the back side of the diode. The interference filter reflects the mid-infrared photons in the range of 2 to 6 microns. The plasma filter reflects the long wavelength radiation starting where the interference filter leaves off.

Figure 4 presents measured reflection for an uncoated plasma filter and an interference filter deposited on a silicon substrate as well as on a plasma filter with a near-infrared (NIR, 0.72-2.5μm) anti-reflection (AR) coatings on the second surface of the substrates. This figure illustrates the respective contributions of the interference filter and the plasma filter.

Conversion efficiencies for single module TPV cells with front surface filters have been previously reported to exceed 20%[2]. Conversion efficiencies for TPV arrays with front surface filters has been reported to exceed 12%[7], with a power density in the range of 0.4 watts/cm^2. These tests were performed using front surface spectral control filters that contained antimony selenide (Sb_2Se_3) as the high index material. Filter designs using this material have energy weighted spectral efficiencies approaching 80%. Spectral efficiency is defined as the ratio of the integrated above band gap power absorbed in the TPV cell to the total power absorbed.

A limitation of Sb_2Se_3 is that it undergoes a phase transformation at elevated temperatures that results in high NIR absorption. In this paper, we present a more detailed discussion of the nature of this absorption, and present alternate film materials that have been demonstrated to withstand higher temperatures.

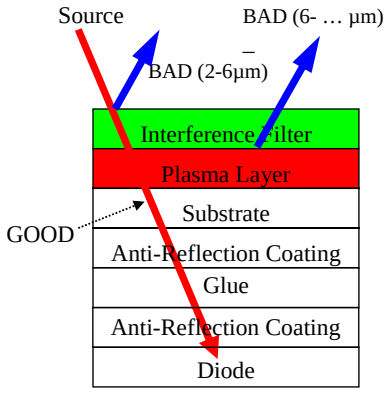

Figure 3: The structure of the TPV direct energy converter and consists of the interference filter deposited on the plasma filter. The InP substrate has an AR film to match the glue used to affix the filter to the TPV cell.

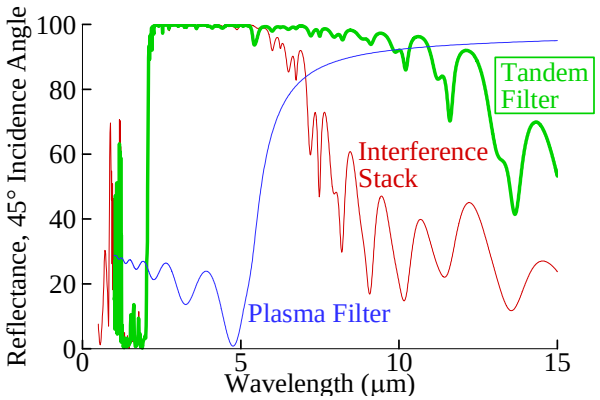

Figure 4: The interference filter defines the transition from high transmission to high reflection and covers the mid-IR region out to 6 microns. The plasma filter provides long wavelength reflection.

2: Front Surface Spectral Control Filters

An interference filter relies on the partial reflection of light from the interface of two materials with different refractive indices. The intensities of the partial reflections from successive interfaces add by superposition, according to the phase of the reflected and incident light. The phase of the light is determined by the order of the index transition (low to high index induces no change in the reflected phase, while high to low shifts the phase by 180°) and the optical thickness of the films. The optical thickness is the product of the refractive index and the physical thickness of the film. If the reflected and incident rays are of the same phase, constructive interference occurs, and the intensity is enhanced. If the phase of the reflected and incident intensity differs by 180°, then destructive interference occurs, and the intensity of the reflected light is reduced. In the example of a quarter-wave notch reflection filter, each repeating group of high and low index materials has an optical thickness of a quarter-wave.

The intensity of the light reflected at an interface is a function of the index contrast or difference between the index values of the materials at the interface. The greater the index contrast, the greater the intensity of reflected light, and the wider the bandwidth of the filter. Since the spectral control filter must cover a broad spectral region, materials of high index contrast result in designs with fewer layers, less total material, and thus less total parasitic absorption, and lower fabrication cost. Figure 5 presents an empirical plot of spectral efficiency versus the refractive index of the high index material for the same basic design. The curve was generated by replacing the index value of the high index material and refining the design keeping the index of the low index material constant. The result is an estimate of the range of spectral efficiency that can be achieved for a design with a particular high index material.

Two observations can be made from Figure 5. The first observation is that the higher the index of the high index material, the higher the spectral efficiency that can be expected. The second observation is that the best performance that can be expected from a front surface filter is

generally bounded by the selection of the high index material, but, in general, will not exceed 90%. A second criterion for the selection of the high index material is that it must have low broadband absorption. Low absorption in the short wavelength region is required for high spectral efficiency and power density, and low absorption in the long wavelength region is also required, since light must pass through the film stack to the plasma filter with minimal absorption if the design is to take advantage of the plasma filter's long wavelength reflection.

The best performing material that has been identified is Sb_2Se_3. The index and absorption values for single material films are presented in Figure 6. These values of n and k were measured using a Wollam Variable Angle Spectral Ellipsometer (VASE). Figure 7 presents measured and expected reflection for a front surface filter fabricated using Sb_2Se_3. The low index material is yttrium fluoride (YF_3).

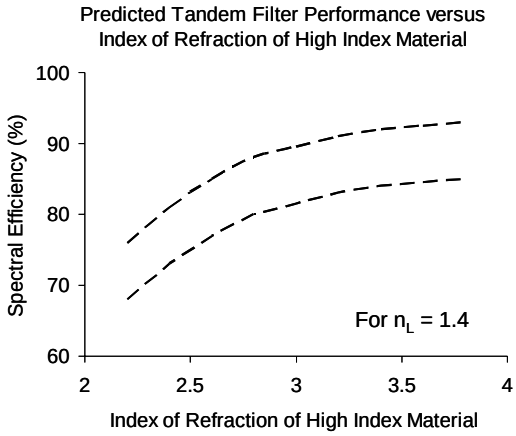

Figure 5: The refractive index of the high index material in a tandem filter design was modified and refined to a reflection target. The results present an empirical estimate of expected performance for the design as a function of the refractive index of the high index material.

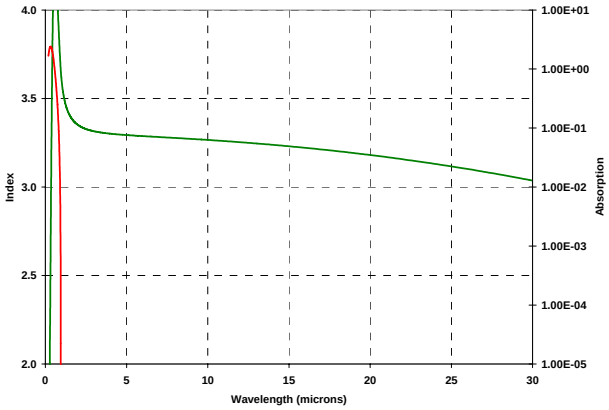

Figure 6: The real (n) and imaginary (k) components of the refractive index of Sb_2Se_3 are presented. The measurements were made from single layer samples of Sb_2Se_3 on silicon and glass using VASE ellipsometry.

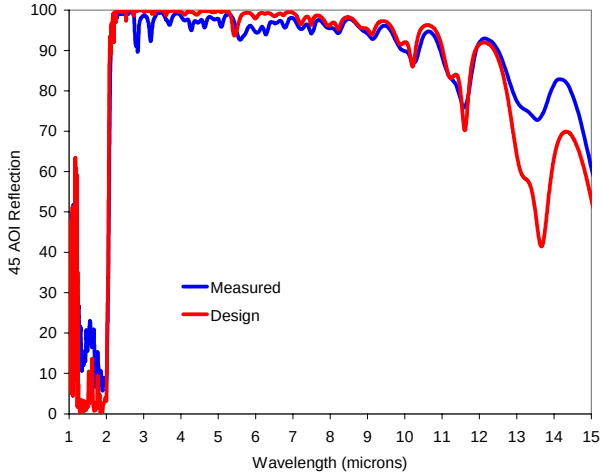

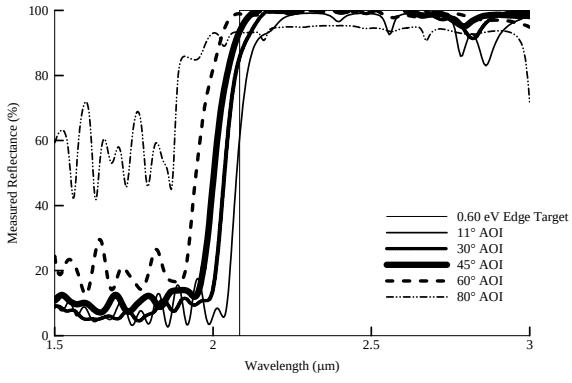

Figure 7: The current front surface filter design is a tandem filter using Sb_2Se_3. A multilayer interference filter is deposited on a solid state plasma reflection filter.

Figure 8: The front surface filter is designed to provide good performance at all angles of incidence. This figure presents measured reflection at a range of incident angles.

Figure 8 presents the measured performance of the front surface tandem filter at a range of angles of incidence (AOI). A key concern in the design of a spectral control filter is that it should perform well over the range of incidence angles determined by the characteristics of the emitter and TPV geometry. For a flat parallel plate emitter and TPV cell geometry, the angle distribution of photon energy at the filter is lambertion[8]. The intensity is peaked at 45°, and falls to zero at normal and 90° AOI. The low reflectance to high reflectance transition of the spectral control filters shifts towards shorter wavelengths with larger angles of incidence[9]. This shift is mitigated by using as high a refractive index material for the film as possible.

3: Material Absorption

Absorption in the materials used to fabricate the front surface filter has a direct impact on the spectral efficiency of the filter, and if that absorption is in the above band gap region, the power density of the cell is also reduced. The current material set for the front surface filters includes YF_3 and Sb_2Se_3. The refractive index of YF_3 is approximately 1.5. The refractive index of Sb_2Se_3 is 3.4. The deposition process for Sb_2Se_3 is such that an amorphous phase of the material results. The advantage of using amorphous Sb_2Se_3 is its high refractive index over a broad spectral range. Unfortunately, NIR absorption increases rapidly when the amorphous Sb_2Se_3 phase is transformed to a crystalline phase when heated.

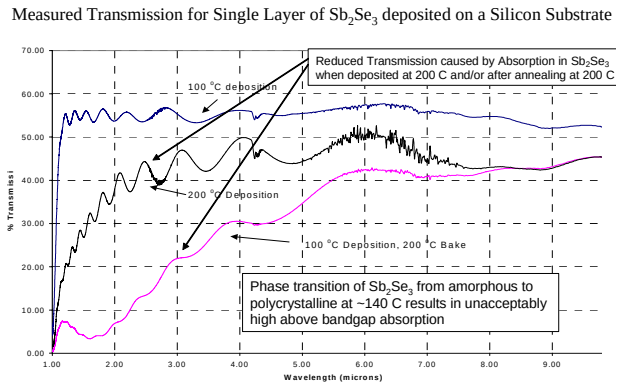

Figure 9: Single layers of Sb_2Se_3 develop significant absorption between 1 and 3 microns when deposited on a hot substrate, or if deposited cold and heated post deposition.

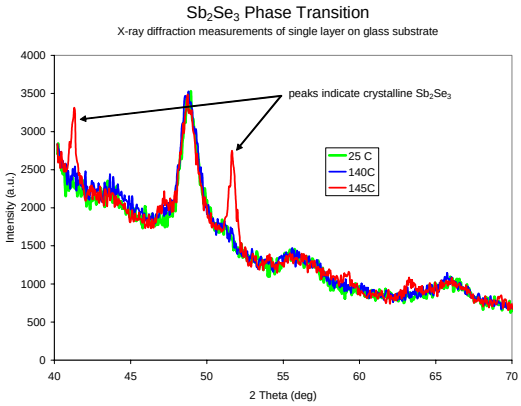

Figure 10: The absorption seems to be related to a phase change which occurs rapidly at or about 145°C.

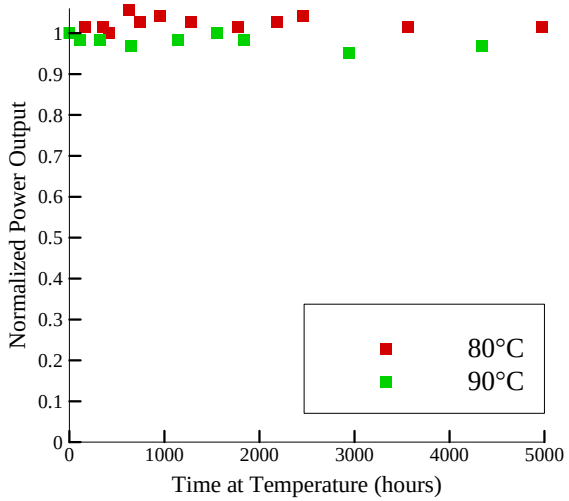

Figure 11: The TPV module with Sb_2Se_3 based filters perform well over time if the temperature is maintained below 90°C.

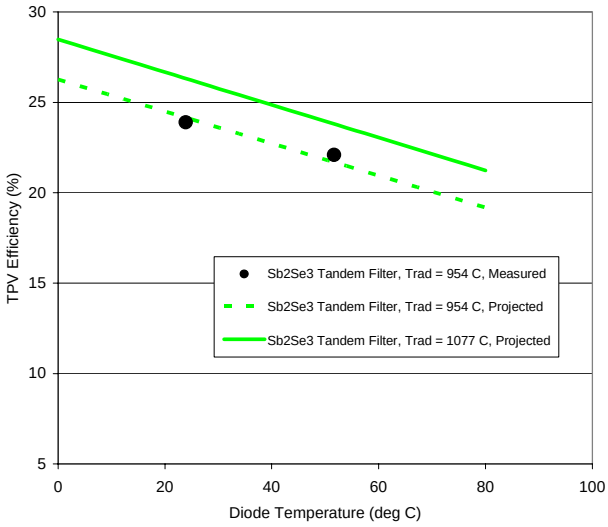

Figure 12: The efficiency of the TPV cells with front surface filters is plotted as a function of the operational temperature of the diode.

Figure 9 presents a plot of measured transmission for a single film sample of Sb_2Se_3 on silicon before and after heating to 200°C. The temperature at which this increase in absorption occurs is more accurately identified in x-ray diffraction measurements presented in Figure 10 as about 145°C. Figure 11 presents results of heating a TPV module with spectral control filter to 80°C and 90°C for extended periods of time. Figure 12 presents TPV performance with a front surface filter as a function of diode temperature. The efficiency of the TPV cell decreases with increased temperature, defining a practical operational range limited to 80 to 90°C. The data in Figure 11 show no degradation in filter or cell performance over time when the module is held at or below a temperature of 90°C. Nevertheless, a temperature excursion could occur, and if it does, the performance of the TPV converter may be compromised depending on the magnitude and duration of the excursion.

4: Alternate Materials

Two alternate high index materials have been identified. These materials are antimony sulfide (Sb_2S_3) and gallium telluride (GaTe). Sb_2S_3 has a refractive index of 2.7 to 2.8. GaTe has a refractive index of 2.9 to 3.1. The higher index of GaTe makes it more attractive for TPV front surface filters than the Sb_2S_3. Figures 13 and 14 present the measured optical constants for Sb_2S_3 and GaTe using VASE ellipsometry. Figures 15 and 16 present x-ray diffraction measurements for the two materials. An amorphous to crystalline phase transformation for Sb_2S_3 is noted at 260°C and at about 290°C for GaTe. Both materials offer substantially higher temperature stability than that measured for Sb_2Se_3.

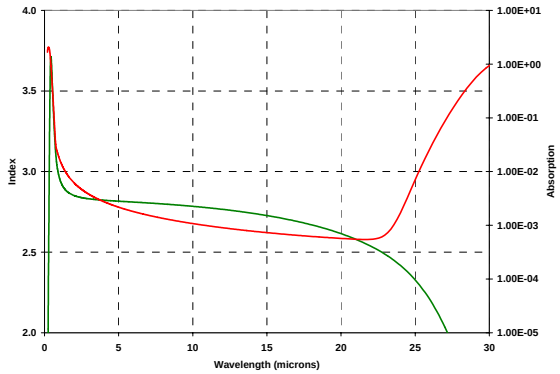

Figure 13: The real (n) and imaginary (k) components of the refractive index of Sb_2S_3 are presented. The measurements were made from single layer samples of Sb_2S_3 on silicon and glass using VASE ellipsometry.

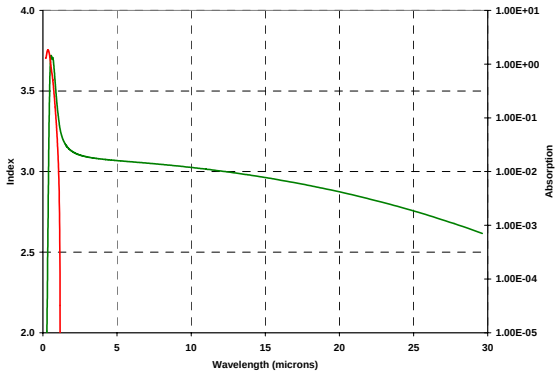

Figure 14: The real (n) and imaginary (k) components of the refractive index of GaTe are presented. The measurements were made from single layer samples of GaTe on silicon and glass using VASE ellipsometry.

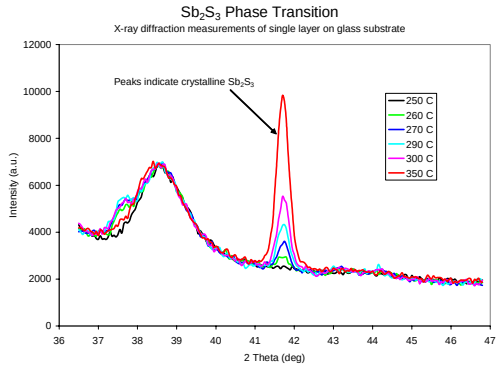

Figure 15: Sb_2S_3 exhibits a phase change at 260°C.

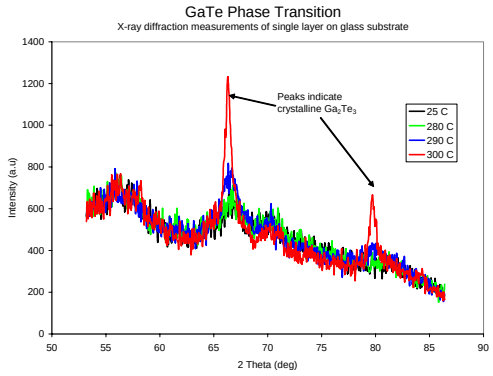

Figure 16: GaTe exhibits a phase change at 290°C.

Filter designs were generated for both materials and are presented in Figures 17 and 18. Filters using both materials were fabricated and shown to be viable. The development focused on the GaTe filters because this material offered higher performance. A comparison of measured and expected (design) reflection for the GaTe filter is presented in Figure 18. GaTe filters have been tested at 150°C for extended periods of time (1583 hours) with no change in spectral performance (Figure 19). Furthermore, measured and projected performance of a TPV module using a GaTe based tandem filter is compared in Figure 20 with TPV measured and projected performance of TPV modules using only a back surface reflector and Sb_2Se_3 based tandem filter. The projected performance of the TPV module with the GaTe based tandem filter is 1-2 percent less than the comparable performance of the TPV module with Sb_2Se_3 based tandem filter. In Figure 20, the measured performance of the TPV module with the GaTe based tandem filter is shown to be slightly higher than the TPV module with Sb_2Se_3 based tandem filter because the TPV module with the GaTe based tandem was measured with a higher radiating surface temperature not because the module has a higher performance than the TPV module with Sb_2Se_3 based tandem.

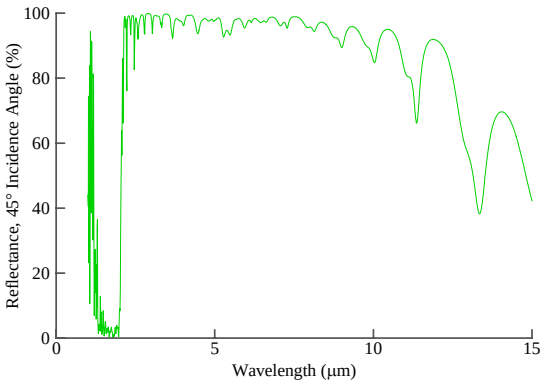

Figure 17: Predicted performance (design) for an antimony sulfide (Sb_2S_3) tandem filter.

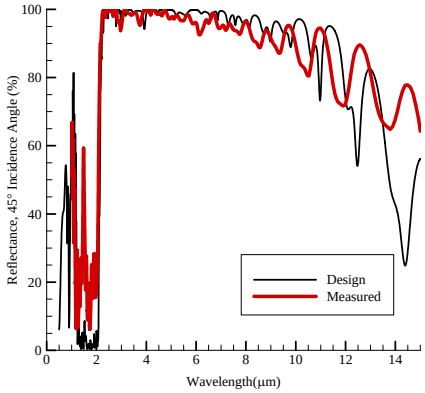

Figure 18: GaTe filters have been fabricated and exhibit good agreement with predicted performance.

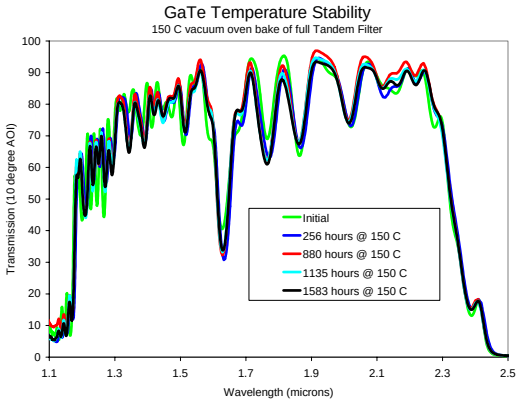

Figure 19: Extended heating of the filter has not resulted in any measureable change in pass band transmission.

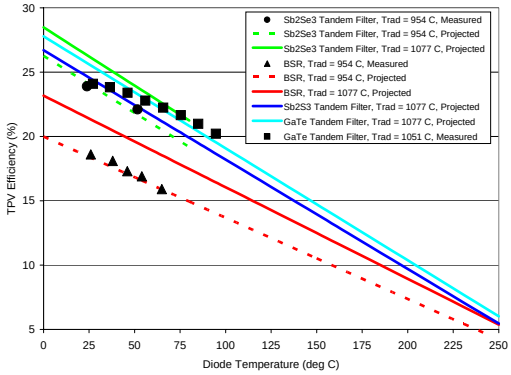

Figure 20: Projected and measured TPV performance versus diode temperature.

Table 1 presents a summary of performance results of filters fabricated using GaTe and YF_3. A total of 27 filters were fabricated. TPV efficiency and power density were calculated from measured spectral reflection at 5 angles. The measurements were input into a system model that includes the performance of the TPV cell, optical adhesive and a back surface reflector (BSR).

Conclusions

Spectral efficiencies in excess of 20% have been measured using for 0.6 eV band gap TPV cells using Sb_2Se_3 front surface tandem filters. Unfortunately, these filters will fail if exposed to temperatures in excess of 90°C. Two alternate high index materials have been identified that offer higher temperature stability. These materials are Sb_2S_3 and GaTe. GaTe has proved the most promising of the two materials, and filters have been fabricating using this material along with YF_3. Further work developing these materials is needed to improve the filter designs and increase the fabrication fidelity to these designs.

Table 1: Summary of GaTe High Index Spectral Control Filters for 0.6 eV Diodes

TPV % Efficiency	Design	20.9
	Mean	17.5
	Std Dev	0.8
	Max	19.0
	Min	15.7
TPV Power Density (W/cm^2)	Design	0.49
	Mean	0.42
	Std Dev	0.024
	Max	0.45
	Min	0.36

References

1. PF Baldasaro, et al. System Performance Projections for TPV Energy Conversion, www.osti.gov.
2. Wernsman, B., et al., Greater than 20% Radiant Heat Conversion Efficiency of a Thermophotovoltaic Radiator / Module System Using Reflective Spectral Control. IEEE Transactions on Electron Devices, 2004. 51(3):p. 512-515.
3. Chubb, D., et al, Spectral Emitters, 1st NREL Conference on Thermophotovoltaic Generation of Electricity, AIP 321,1995, pp 229-244.
4. Fourspring, P. M., et al. Thermophotovoltaic Spectral Control, CP738, Thermophotovoltaic Generation of Electricity, pp 171-179.6th Conference, 2004 AIP 0-7354-0222-1/04.
5. Rahmlow, T., et al, New Performance Levels for TPV Front Surface Filters, pp 181- 188, CP738, Thermophotovoltaic Generation of Electricity, 6th Conference, 2004 AIP 0-7354-0222-1/04.
6. Charache, G.,Theoretical prediction of the plasma frequency and Moss-Burstein shifts for degenerately doped In{sub x}Ga{sub 1{minus}x}As, J. Applied Physics, V86, 1999.
7. Burger, S., Brown, E., Rahner, et al. Thermophotovoltaic Array Optimization, 2004 Jul 29, www.osti.gov.
8. Siegel, R and Howell, J., Thermal Radiation Heat Transfer, Taylor & Francis, Inc., 2001.
9. Macleod, H. A., Thin Film Optical Filters, 2nd Ed, 1989, McGraw-Hill.